The CBL-CIPK Network Integrates Calcium and ABA Signaling to Mediate Drought Adaptation in Asparagus cochinchinensis

Zhengxi Long
School of Life Sciences/Key laboratory of Plant Resource Conservation and Germplasm Innovation in Mountainous Region (Ministry of Education), Guizhou University
Liu Tang
School of Life Sciences/Key laboratory of Plant Resource Conservation and Germplasm Innovation in Mountainous Region (Ministry of Education), Guizhou University
Shengbo Lu
Qiannan Academy of Agricultural Sciences (The academy of Duyun Maojian tea)
Yuting Yang
Qiannan Academy of Agricultural Sciences (The academy of Duyun Maojian tea)
Mingsheng Zhang
School of Life Sciences/Key laboratory of Plant Resource Conservation and Germplasm Innovation in Mountainous Region (Ministry of Education), Guizhou University
miao liu
Miaoliu1991@163.com
School of Life Sciences/Key laboratory of Plant Resource Conservation and Germplasm Innovation in Mountainous Region (Ministry of Education), Guizhou University

Research Article

Keywords: Asparagus cochinchinensis, Drought stress, Full-length transcriptome, CBL-CIPK network, ABA signaling

Posted Date: February 14th, 2026

DOI: https://doi.org/10.21203/rs.3.rs-8784662/v1

Additional Declarations: No competing interests reported.

Abstract

Background

Asparagus cochinchinensis (Lour.) Merr. (*A. cochinchinensis*) is a precious traditional Chinese medicinal herb with significant economic value. However, its cultivation is severely constrained by environmental stresses, particularly drought. The Calcineurin B-Like (CBL) and CBL-Interacting Protein Kinase (CIPK) network constitutes a crucial calcium sensor system that decodes stress-induced Ca^{2+} signatures in plants. Despite its importance, the molecular architecture and functional roles of the CBL-CIPK network in *A. cochinchinensis* remain largely uncharacterized.

Results

In this study, we generated a high-quality full-length transcriptome of *A. cochinchinensis* using PacBio Single-Molecule Real-Time (SMRT) sequencing, yielding 52,042 non-redundant transcripts. Based on this resource, we identified 35 *AcCIPK* and 13 *AcCBL* genes. Phylogenetic analysis revealed high conservation between *AcCIPK24/AcCIPK23* and their Arabidopsis orthologs, while also uncovering species-specific alternative splicing events, including a truncated isoform of *AcCIPK24.5*. Yeast two-hybrid assays confirmed a specific physical interaction between AcCBL10 and AcCIPK24. Expression profiling demonstrated that these genes exhibit tissue-specific and temporal responses to drought stress. Notably, while both genes were downregulated in roots and stems under drought, *AcCBL10* was significantly upregulated in cladodes, suggesting complex regulatory mechanisms. Furthermore, hormone analysis revealed that drought stress induced endogenous ABA accumulation, and exogenous ABA application not only accelerated this peak but also enhanced the expression of *AcCBL10* and *AcCIPK24.5*, indicating a positive feedback loop between calcium signaling and ABA pathways.

Conclusion

This study provides the first comprehensive functional characterization of the CBL-CIPK network in *A. cochinchinensis*. The specific interaction between *AcCBL10* and *AcCIPK24*, coupled with the crosstalk between calcium signaling and ABA pathways, highlights a key molecular mechanism underlying drought adaptation in this medicinal plant.

1. Introdution

Calcium ions (Ca^{2+}) act as ubiquitous intracellular secondary messengers, integrating signaling pathways essential for plant growth, development, and stress responses (Zhang et al., 2022; Zhu et al., 2022). Specific sensor proteins, such as the plant-specific calcineurin B-like (CBL) family, detect these cytosolic Ca^{2+} concentration fluctuations (Zhou et al., 2015). CBL proteins contain four conserved EF-hand domains that bind Ca^{2+}, enabling them to decode Ca^{2+} signals (Verma et al., 2021). These proteins selectively interact with CBL-interacting protein kinases (CIPKs), forming CBL-CIPK complexes that serve as central components of Ca^{2+} signal transduction (Zhang et al., 2020).

The subcellular localization of CBL determines its functional specificity, which is primarily governed by distinct N-terminal targeting sequences (Tang et al., 2020). The classical (type I) CBL contains a dual lipid modification motif (MGCXXS/T) and localizes to the plasma membrane (Weinl et al., 2009). The tonoplast-type (type II) CBL harbors a tonoplast targeting sequence (TTS) (Xu et al., 2006). The membrane-anchored (type III) CBL possesses a transmembrane helix domain that enables its localization to either the tonoplast or plasma membrane (Tang et al., 2020; Waadt et al., 2008). The interaction with CIPK is mediated by a shared C-terminal PFPF/FPSF motif containing a profound phosphorylation site that is essential for complex regulation (Aslam et al., 2019).

CIPK contains an N-terminal serine/threonine kinase domain and a C-terminal regulatory domain (Shi et al., 2021). The regulatory domain features a highly conserved NAF/FISL motif (core residues: N, A, F, I, S, L) that functions both as the primary CBL-binding site and as an autoinhibitory domain (Wu et al., 2024). When Ca^{2+}-activated CBL binds to this motif, it releases autoinhibition and activates the CIPK kinase domain in a calcium-dependent manner (Xiao et al., 2022). Some CIPKs also possess a less conserved protein phosphatase interaction site (PPI) adjacent to the NAF/FISL motif, potentially facilitating interactions with phosphatase regulators like ABI/PP2Cs (Yu et al., 2014).

Plants inhabiting specific ecological niches, particularly those in karst regions like *A. cochinchinensis*, face unique water scarcity challenges due to the high permeability of limestone substrates. This medicinally important herb has evolved sophisticated mechanisms to cope with the fluctuating water availability in such environments. Given that calcium signaling is often the first responder to osmotic changes, it is hypothesized that the CBL-CIPK network in *A. cochinchinensis* may have undergone specific evolutionary adaptations to fine-tune its drought response. The CBL-CIPK signaling network plays a crucial role in regulating diverse physiological processes across the plant life cycle. This system mediates plant responses to multiple abiotic stresses, such as salinity, drought, low temperature, and heavy metal exposure (Kanwar et al., 2014; Ma et al., et al., 2020; Kaya et al., 2024). It also governs essential developmental stages including seedling establishment, flowering initiation, root architecture, pollen germination, and pollen tube elongation (Wang et al., 2020). Recent studies have further demonstrated its involvement in phytohormone pathways, particularly through interactions with ABA signaling, GA biosynthesis, and cold stress adaptation mechanisms (Kolukisaoglu et al., 2004).

Drought stress severely limits plant growth, development, and agricultural productivity by disrupting water homeostasis, inducing osmotic stress, and impairing metabolic functions (González et al., 2023). Plants detect water deficit and activate adaptive responses, with the evolutionarily conserved CBL-CIPK signaling module serving as a key decoder of stress-induced Ca^{2+} fluxes and playing a critical role in drought adaptation (Cheong et al., 2007). This complex regulates ion homeostasis by directly modulating plasma membrane and tonoplast ion channels and transporters (e.g., K^+ channels, H^+-ATPases), thereby controlling essential drought tolerance mechanisms (Apse et al., 1999; Tang et al., 2015). The module also coordinates diverse cellular responses, such as osmoprotectant accumulation and hormone signaling pathway regulation. Studies across multiple plant species have demonstrated that specific CBL-CIPK interactions are indispensable for drought resistance. Overexpressing *AtCIPK1/23*, *AtCBL1/9*, *OsCIPK3/12/15*, and *MdCIPK22* enhances drought tolerance in Arabidopsis, rice, and apple, while loss-of-function mutants (e.g., *cipk1*, *cbl1*) show increased drought sensitivity (Cho et al., 2018; Ma et al., 2019., Gao et al., 2019; Lara et al., 2020; Peng et al., 2021; Chao et al., 2022). These findings suggest that genetic manipulation of this signaling pathway could effectively improve crop drought resilience.

A. cochinchinensis, a highly valued traditional Chinese medicinal herb renowned for its therapeutic properties, often faces cultivation challenges due to various environmental stresses (Wang et al., 2022; Yunmam et al., 2023). Although the medicinal properties and genomic resources of *A. cochinchinensis* have been recently advanced, the composition, structural diversity (such as alternative splicing variants), and functional specificity of the CBL-CIPK network in this species remain largely elusive. Furthermore, the crosstalk between the CBL-CIPK cascade and phytohormone signaling, particularly Abscisic Acid (ABA), which is central to drought adaptation, has not been elucidated in this non-model medicinal plant.

In this study, we performed full-length transcriptome sequencing to generate a comprehensive genomic resource. We systematically identified and characterized the *CBL* and *CIPK* gene families, with a specific focus on evolutionary conservation and structural divergence. Furthermore, we validated the specific protein-protein interaction between key drought-responsive modules (AcCBL10 and AcCIPK24) and investigated their expression dynamics under drought stress. Our work aims to decipher the molecular architecture of the CBL-CIPK network and its interaction with ABA signaling, providing novel insights into the drought adaptation mechanisms of *A. cochinchinensis*.

2. Materials and Methods

2.1 Sample Collection and Processing

In this experiment, the tested *A. cochinchinensis* samples were collected from Danzhai County (107°44'-108°08'E, 26°05'-26°26'N), Qiandongnan Prefecture, Guizhou Province, and authenticated by Professor Zhang Mingsheng, the Chief Scientist of Guizhou Province. The roots, stems, cladodes, flowers, and fruits of *A. cochinchinensis* were mixed, flash-frozen in liquid nitrogen, and stored at -80°C to ensure sample stability and subsequent experimental accuracy (Hajihashemi et al., 2018). The experiment was designed with three biological replicates to enhance the reliability and reproducibility of the results.

For drought stress assays, *A. cochinchinensis* materials were cultivated in the greenhouse of Guizhou University and subjected to continuous treatment with 20% PEG6000 for 0, 2, 6, 12, and 24 h. The underground tissues were then collected for RNA extraction. Throughout the sampling period, water was replenished regularly to maintain PEG6000 concentration (Yao et al., 2022). Each treatment group consisted of three independent biological replicates, with 10 plants per replicate.

Design specific primers (primer sequence shown in Table S1), using the internal reference gene Actin as a control, and calculate the relative expression levels of different tissues and organs as well as after drought stress treatment using the $2^{-\Delta\Delta Ct}$ method.

2.2 RNA extraction, sequencing library construction and sequencing assembly

Total RNA was isolated from tissue samples with TRIzol reagent (Life Technologies). The Agilent 2100 Bioanalyzer, agarose gel electrophoresis, and NanoDrop 2000 spectrophotometer confirmed RNA integrity (RIN ≥ 8.0), purity (OD260/280 = 1.8-2.0; OD260/230 ≥ 2.0), and concentration. Using the SMARTer approach (NEBNext® Single Cell/Low Input RNA Library Prep Kit), qualified RNA samples underwent double-stranded cDNA synthesis, PCR amplification, end repair, and PacBio SMRTbell adapter ligation (Cheng et al., 2019). The PacBio Sequel II platform sequenced quality-verified libraries by single-molecule real-time (SMRT) technology, achieving a target yield of ≥8Gb per sample. SMRT Link v10.2 produced circular consensus sequences (CCS, ≥3 full passes), from which full-length transcripts were identified by the presence of both 5'-primer (GCAATGAAGTCGCAGGGTTG) and 3'-primer (AAGCAGTGGTATCAACGCAGAGT). The iterative clustering and error correction (ICE) algorithm generated consensus sequences with ≥0.99 predicted accuracy for downstream analysis (Wang et al., 2023).

2.3 Annotation of full-length transcript

The full-length transcript was aligned with the NCBI non-redundant proteins database (NCBI non-redundant proteins, Nr, http://www.ncbi.nlm.nih.gov), Swiss-Prot protein database (Swiss-Prot protein database, http://www.expasy.ch/sprot), Kyoto encyclopedia of genes and genomes database (KEGG, http://www.genome.jp/kegg), and COG/KOG database (COG/KOG database, http://www.ncbi.nlm.nih.gov/COG) using BLASTX alignment, with an E-value threshold set at 1E-5, to assess the sequence similarity between the full-length transcript of Asparagus and that of *Asparagus cochinchinensis*, and obtain basic annotations for each full-length transcript (Ning et al., 2024). Blast2GO software was used to perform GO annotation analysis on the Nr annotation results of the full-length transcript (Conesa et al., 2005). WEGO software was utilized for hierarchical functional classification of the full-length transcript (Ye et al., 2018).

2.4 Transcriptome structural feature analysis and gene function prediction

The Astalavista software identified alternative splicing patterns in precursor mRNA (pre-mRNA) transcribed from each gene. We performed genome-wide simple sequence repeat (SSR) mining with the MicroSAtellite identification tool (MISA), applying these parameters: 1-12, 2-6, 3-5, 4-5, 5-4, and 6-4. SSRs separated by less than 100 bp were merged and treated as a single locus (Tandon et al., 2023). TransDecoder (v3.0.0) predicted reliable coding sequence (CDS) regions from transcript sequences by evaluating open reading frame (ORF) length, log-likelihood scores, and alignment of amino acid

sequences against Pfam protein domains (Ramos et al., 2021). For novel transcripts, we predicted long non-coding RNAs (lncRNAs) by combining four computational approaches: Coding Potential Calculator (CPC), Coding-Non-Coding Index (CNCI), Pfam domain analysis, and Coding Potential Assessment Tool (CPAT). Transcripts were classified as lncRNAs only when all four methods agreed on their non-coding status (Duan et al., 2021).

2.5 Transcription Factor Analysis and Functional Annotation of Novel Transcripts

Transcription factors (TFs) in *A. cochinchinensis* were identified using iTAK (http://itak.feilab.net/cgi-bin/itak/index.cgi), with subsequent validation using hmmscan to align query sequences against the Pfam database for TF quantification (Zheng et al., 2016). Following deduplication, gffcompare analyzed full-length transcripts in GFF3 format against the reference genome's annotations. The study detected novel transcripts and genes absent from the reference genome, which were then functionally annotated by DIAMOND (v2.0.15) through alignment with NR, SwissProt, GO, COG, KOG, Pfam, and KEGG databases (Sun et al., 2021).

2.6 Identification of the *CBL* and *CIPK* Gene Families in *A. cochinchinensis*

Candidate genes were screened from the full-length transcriptome of *Asparagus cochinchinensis* (*A. cochinchinensis*) through BLASTP alignment against protein sequences of AtCBLs (e.g., AT4G17615) and AtCIPKs (e.g., AT3G17510) in *A. thaliana*, as well as those of *A. cochinchinensis* (Table S1). The conserved domains of CBL (PF00036 and PF13499) and CIPK (PF00069 and PF03822) were searched using HMMER 3.3, and domain integrity was further verified with the SMART database (Wu et al., 2023). A neighbor-joining tree was constructed using MEGA 12 with the p-distance model and 1000 bootstrap replicates.

2.7 Secondary and tertiary structure analysis of AcCBLs and AcCIPKs

Conserved motifs in the AcCBL and AcCIPK protein sequences were identified using the MEME (v4.12.0; http://meme-suite.org/tools/meme), configured to detect up to 15 motifs with an optimum width of 6 - 200 residues. Only motifs satisfying a stringent significance threshold (e-value ≤ 1e-10) were retained. The motif distribution patterns were visualized with TBtools (Huang et al., 2022). We computationally characterized the AcCBL and AcCIPK proteins using the following tools: ExPASy for physicochemical properties, TMPRED for predicting transmembrane domains, SignalP 4.1 for identifying signal peptides, and Plant-mPLoc for inferring subcellular localizations (Wu et al., 2023). The tertiary structures of CBL and CIPK family members from *A. cochinchinensis* were predicted using the I-TASSER platform (Biasini et al., 2014).

2.8 Yeast Two Hybrid

The yeast two-hybrid (Y2H) assay utilized the Saccharomyces cerevisiae strain Y2HGold, where AcCBL10 was cloned into pGADT7 as the prey and AcCIPK23/24 into pGBKT7 as the bait (Li et al., 2016). The positive control featured pGADT7-T co-transformed with pGBKT7-53, whereas pGADT7-T combined with pGBKT7-lam constituted the negative control. To assess transcriptional self-activation, pGADT7 was separately co-transformed with either pGBKT7-AcCBL10 or pGBKT7-AcCIPK23/24. All primer sequences are listed in Table S3 (Yang et al., 2013). The optimal 3-AT concentration for suppressing background growth was determined by culturing Y2HGold cells harboring the bait plasmid on dropout media (DDO, TDO, and QDO) containing a gradient of 3-AT concentrations at 30 °C for five days. Protein-protein interactions were confirmed by plating co-transformed Y2HGold cells on DDO, TDO supplemented with 15 $mmol \cdot L^{-1}$ 3-AT, and QDO media, followed by incubation under the same conditions (Huang et al., 2023).

2.9 Plant Growth Conditions and Drought Stress Treatments

The tissue culture seedlings of *A. cochinchinensis* were preserved at the Key Laboratory of Plant Resources Conservation and Germplasm Innovation in Mountainous Region, Guizhou University. Uniform and robust tissue-cultured seedlings were selected for transplanting. The cultivation substrate was a mixture of peat soil and perlite at a 3:1 ratio. The plants were

maintained under conditions of approximately 95% relative humidity, a temperature of 20-28 °C, and no direct light. After one month of soil cultivation, uniformly growing and healthy plants were selected for the simulated drought treatment experiment. The experiment included two treatments: one group was treated with a 1/2 Hoagland nutrient solution containing 20% (w/v) PEG 6000 to simulate drought stress (Yao et al., 2022); the other group was treated with a 1/2 Hoagland nutrient solution containing both 20% (w/v) PEG 6000 and 100 mM ABA for a combined PEG and ABA treatment (Wu et al., 2019). A control group (CK) was set up using the basic 1/2 Hoagland nutrient solution under normal light/dark cycles. Each treatment had three biological replicates, with each replicate consisting of ten seedlings. Samples were collected at 0, 3, 6, and 12 hours after treatment, immediately frozen in liquid nitrogen, and stored for subsequent RNA extraction and analysis.

3. Results

3.1 Full-Length Transcriptome Assembly and Quality Assessment

High-quality full-length transcripts were generated using PacBio Sequel II sequencing, yielding 12.6 Gb of raw data. After adapter trimming and quality filtering, 340,429 circular consensus sequences (CCS) were obtained. Among these, 307,748 reads (90.4%) contained intact 5’/3’ primers and poly A tails and were classified as full-length non-chimeric (FLNC) reads (Fig. S1A). Clustering the FLNC reads yielded 118,501 high-quality consensus isoforms (accuracy > 99%), and subsequent dereplication using cDNA_Cupcake resulted in 52,042 non-redundant transcripts with an N50 of 2.9 kb (Fig. S1B). BUSCO v3.0.2 analysis against the plantae_odb10 database assessed assembly completeness, recovering 94.2% of core genes (2.1% fragmented, 3.7% missing) and confirming high assembly integrity (Fig. S2). BLASTN analysis further validated the assembly by demonstrating 92.3% sequence identity with the *A. cochinchinensis* reference genome.

3.2 Functional Annotation of Transcripts

Comprehensive annotation of the 52,042 non-redundant transcripts against multiple public databases successfully assigned functions to 37,827 (72.7%) transcripts in at least one database. Homology searches revealed that 37,794 (72.6%) transcripts had significant matches in the NR database, with the highest similarity to *A. cochinchinensis* (~71.5%), followed by *Phoenix dactylifera* and *Elaeis guineensis* (Fig. S3A). A total of 29,211 (56.1%) transcripts were matched to the manually curated Swiss-Prot database. Gene Ontology (GO) terms were assigned to 32,892 (63.2%) transcripts, which were predominantly enriched in the biological process categories of 'cellular process', 'metabolic process', and 'response to stimulus' (Fig. S3B). KEGG pathway analysis associated 29,388 transcripts (56.5%) with various pathways and identified 134 enriched pathways, providing a foundation for further investigation into Asparagus biological metabolism and its metabolic network (Table S1). Cluster of Orthologous Groups (COG/KOG) analysis classified 26,188 (50.3%) transcripts into 25 functional categories, where 'General function prediction only' (15.8%), 'Posttranslational modification, protein turnover, chaperones' (11.2%), and 'Signal transduction mechanisms' (10.5%) were the most abundant (Fig. S3C). Pfam domain analysis identified domains in 31,513 (60.6%) transcripts, with protein kinase, leucine-rich repeat, and EF-hand domains being the most prevalent.

3.3 Structural Characterization of Novel Transcripts

In-depth transcriptome analysis identified 38,352 novel transcripts absent from the current reference annotation. A total of 31,724 simple sequence repeats (SSRs) were detected within 21,374 transcripts, with mononucleotide repeats (48.0%) being the most frequent, followed by di- (26.8%) and tri-nucleotide (23.3%) repeats (Fig. S4A). TransDecoder predicted 37,684 open reading frames (ORFs), of which 28,366 (75.3%) were complete, containing both start and stop codons (Fig. S4B). Alternative splicing (AS) analysis revealed extensive mRNA isoform diversity, identifying 13,580 gene loci and 1,382 novel loci. We cataloged 5,874 AS events, with intron retention (IR, 34.1%) and exon skipping (ES, 28.7%) representing the predominant types (Fig. S4C). Furthermore, 521 potential fusion transcripts were predicted, suggesting possible gene rearrangements or trans-splicing events.

3.4 Identification and Functional Prediction of LncRNAs

A stringent pipeline integrating four computational tools (CPC2, CNCI, CPAT, and Pfam scan) identified 366 high-confidence long non-coding RNAs (LncRNAs) (Fig. S5A). These lncRNAs were classified according to their genomic context relative to protein-coding genes, with 58.7% designated as intergenic (lincRNAs), 21.3% as antisense, 12.0% as intronic, and 8.0% as sense overlapping (Fig. S5B). Target gene prediction, based on both cis-regulation (genomic proximity) and trans-regulation (sequence complementarity), indicated that these lncRNAs may regulate genes associated with transcription, stress response, and metabolic processes.

3.5 Transcription Factor Family Analysis

Comprehensive analysis with the iTAK pipeline identified 7,565 transcripts encoding transcription factors (TFs) and transcriptional regulators (TRs), accounting for 14.5% of all transcripts. These TFs were classified into 58 distinct families. The most abundant families were bHLH (9.2%), ERF (8.5%), MYB-related (7.1%), NAC (6.3%), and C2H2 (5.8%), all of which are known to be critically involved in plant development, hormone signaling, and responses to abiotic stress (Fig. S6).

3.6 Genome-wide characterization of CBL-CIPK networks

In order to comprehensively identify the CIPK and CBL genes in the full-length transcriptome data of Asparagus, the bidirectional BLAST method was used for identification. Members were named 48 members such as AcCIPK1 and AcCBL1 according to the genetic distance between them and the members of the Arabidopsis CIPK and CBL gene family (Table 1).

The basic characteristics of gene coding sequence (CDS), protein molecular weight (MW), isoelectric point (PI) and subcellular localization were analyzed. Among the 35 identified CIPK protein members, their protein lengths ranged from 296 amino acids (aa) (AcCIPK24.3) to 485 aa (AcCIPK3.7), with corresponding molecular weights of 33,664.73 kDa (AcCIPK24.3) and 55,500.55 kDa (AcCIPK3.7), respectively. The CIPK family included 11 acidic proteins and 24 basic proteins, with isoelectric points (pI) distributed between 4.98 and 9.28. Subcellular localization analysis revealed that, with the exception of AcCIPK1.1, the remaining 34 members were localized to the cytoplasm. Notably, AcCIPK23.2 and AcCIPK23.3 were also predicted to localize to the cytoplasm. Among the 13 identified CBL protein members, protein lengths spanned from 64 aa (AcCBL4.2) to 283 aa (AcCBL9), with corresponding molecular weights ranging from approximately 7.17 kDa (AcCBL4.2) to 33.01 kDa (AcCBL9). The isoelectric points ranged from 4.51 (AcCBL4.2) to 5.23 (AcCBL9), and all members were acidic proteins. Subcellular localization results indicated diverse localization patterns for these 13 CBL members, including the nucleus (AcCBL2.1, AcCBL2.2), plasma membrane (AcCBL3.1, AcCBL3.2, AcCBL4.1, AcCBL8, AcCBL9, AcCBL10), and endoplasmic reticulum (AcCBL3.5), among others (Table 1).

Table 1. List of *CIPK* and *CBL* Family Genes Identified in *A. cochinchinensis*

Gene ID in *A. cochinchinensis*	Gene Name in *A. cochinchinensis*	Gene ID in *A. thaliana*	Gene Name in *A. thaliana*	Protein Length (aa)	Molecular Weight (kDa)	Protein Isoelectric Point (pI)	Protein Subcellular Localization
PB.8729	AcCIPK1	AT3G17510	AtCIPK1	446	50452.39	6.68	Nucleus
PB.11531.2	AcCIPK2.1	AT5G45820	AtCIPK2	456	52218.28	9.24	Cytoplasm
PB.1938.3	AcCIPK2.2			458	52116.97	8.79	Cytoplasm
PB.1938.5	AcCIPK2.3			458	52116.97	8.79	Cytoplasm
PB.2547.1	AcCIPK3.1	AT2G26980	AtCIPK3	436	49817.34	7.62	Cytoplasm
PB.2547.4	AcCIPK3.2			268	30751.96	4.98	Cytoplasm
PB.2547.6	AcCIPK3.3			441	50338.87	6.79	Cytoplasm
PB.2547.7	AcCIPK3.4			441	50352.89	6.79	Cytoplasm
PB.2547.8	AcCIPK3.5			474	54324.46	8.03	Cytoplasm
PB.2547.9	AcCIPK3.6			441	50398.97	6.79	Cytoplasm
PB.8993.3	AcCIPK3.7			485	55500.55	7.59	Cytoplasm. Nucleus.
PB.8993.4	AcCIPK3.8			360	41035.43	5.14	Cytoplasm
PB.2547.10	AcCIPK3.9			441	50398.97	6.79	Cytoplasm
PB.12492.1	AcCIPK9.1	AT1G01140	AtCIPK9	435	49466.56	8.37	Cytoplasm
PB.5252.1	AcCIPK9.2			358	40900.47	6.77	Cytoplasm
PB.5252.2	AcCIPK9.3			436	49601.67	8.44	Cytoplasm
PB.5252.5	AcCIPK9.4			372	42311.32	6.44	Cytoplasm
PB.8410.7	AcCIPK10.1	AT5G58380	AtCIPK10	458	51650.75	9.20	Cytoplasm
PB.8410.6	AcCIPK10.2			458	51635.70	9.20	Cytoplasm
PB.5949.3	AcCIPK10.3			454	51336.75	9.28	Centrosome Cytoplasm Nucleus
PB.5949.4	AcCIPK10.4			374	42197.81	8.92	Cytoplasm Nucleus
PB.8410.1	AcCIPK10.5			458	51635.70	9.20	Cytoplasm
PB.8410.3	AcCIPK10.6			458	51650.75	9.20	Cytoplasm
PB.8410.4	AcCIPK10.7			354	39582.45	8.17	Cytoplasm
PB.8410.5	AcCIPK10.8			458	51650.75	9.20	Cytoplasm
PB.8137.6	AcCIPK23.1	AT1G30270	AtCIPK23	369	41492.54	6.25	Cytoplasm. Nucleus.
PB.8137.1	AcCIPK23.2			445	50030.64	8.90	Centrosome Cytoplasm Nucleus

PB.8137.3	AcCIPK23.3			445	50030.64	8.90	Centrosome Cytoplasm Nucleus
PB.8137.4	AcCIPK23.4			390	44079.77	7.63	Cytoplasm.
PB.8137.5	AcCIPK23.5			365	41565.23	9.04	Cytoplasm Nucleus
PB.7948.1	AcCIPK24.1	AT5G35410	AtCIPK24	442	49949.86	8.56	Cytoplasm.
PB.7948.3	AcCIPK24.2			422	47407.46	8.58	Cytoplasm. Nucleus.
PB.7948.4	AcCIPK24.3			296	33664.73	6.19	Nucleus
PB.7948.6	AcCIPK24.4			393	44592.75	8.86	Cytoplasm
PB.7948.8	AcCIPK24.5			398	44525.02	7.68	Cytoplasm
PB.6643.1	AcCBL2.1	AT5G55990	AtCBL2	80	9184.37	4.68	Nucleus
PB.6643.2	AcCBL2.2			80	9184.37	4.68	Nucleus
PB.295.4	AcCBL3.1	AT4G26570	AtCBL3	224	25757.43	4.83	Cell membrane
PB.6643.4	AcCBL3.2			206	23602.97	4.76	Cell membrane. Cytoplasm
PB.295.5	AcCBL3.3			148	16919.75	5.22	Extracell
PB.295.6	AcCBL3.4			111	12608.98	5.03	Extracell. Nucleus.
PB.295.3	AcCBL3.5			168	19356.32	4.79	Endoplasmic reticulum
PB.6530.4	AcCBL4.1	AT5G24270	AtCBL4	214	24563.29	5.06	Cell membrane
PB.6530.2	AcCBL4.2			64	7168.26	4.51	Cytoplasm. Nucleus.
PB.295.1	AcCBL5	AT4G01420	AtCBL5	94	10835.59	4.82	Extracell
PB.6530.1	AcCBL8	AT1G64480	AtCBL8	214	24563.29	5.06	Cell membrane
PB.10318.1	AcCBL9	AT5G47100	AtCBL9	283	33008.04	5.23	Cell membrane. Extracell
PB.4106.1	AcCBL10	AT4G33000	AtCBL10	170	19606.24	4.99	Cell membrane. Cytoplasm

Most members clustered separately due to species differences, but CIPK3, CIPK9, CIPK23, and CIPK24 grouped into a single clade in Arabidopsis and *A. cochinchinensis* (Fig 1A$_1$). Similarly, AcCBL10 and AtCBL10 exhibited a close phylogenetic relationship. Based on these findings, it is hypothesized that the copies of these genes in *A. cochinchinensis* may possess functions similar to those of their homologs in Arabidopsis (Fig 1B$_1$). Regarding motif distribution, members within the same clade shared similar motif compositions. Specifically, the motif compositions of AcCIPK23.2 and AcCIPK23.3 were identical to that of AtCIPK23.2, and the motif composition of AcCIPK24.1 was the same as that of AtCIPK24 (Fig 1A$_2$). In addition, AcCBL10 lacked only motif14 compared with AtCBL10 (Fig 1B$_2$). These results suggest

that the CIPK23, CIPK24 and CBL10 proteins are relatively conserved in terms of structural and functional integrity during evolution.

3.7 Tissue-Specific Expression Analysis of *AcCIPK* and *AcCBL* Genes under Drought Stress

In plants, CBL-CIPK complexes are key signaling modules in drought responses (Arab et al., 2023). To investigate the potential functions of the key genes identified in this study in the drought response of *A. cochinchinensis*, seven representative genes, including *AcCIPK24.5* and *AcCBL10* were selected. Their expression dynamics in root, stem, and cladode under both normal and drought conditions were analyzed using qRT-PCR.

The results indicated that drought stress significantly affected the expression levels of most tested genes, and this regulatory role exhibited distinct tissue specificity (Fig 2). In roots, the expression of *AcCIPK10.3*, *AcCIPK10.4*, *AcCIPK24.5*, *AcCBL10*, and *AcCIPK2.1* was significantly suppressed by drought ($P < 0.05$), with *AcCIPK2.1* showing the greatest downregulation. In contrast, the expression of *AcCIPK10.8* and *AcCIPK9.3* showed no significant change. In stem, the expression of *AcCIPK10.3*, *AcCIPK10.4*, *AcCIPK10.8*, and *AcCBL10* was significantly downregulated by drought, while *AcCIPK9.3* expression was significantly induced. The expression of *AcCIPK24.5* and *AcCIPK2.1* remained relatively stable. In cladodes, the expression of *AcCIPK10.8*, *AcCIPK24.5*, and *AcCBL10* was significantly downregulated by drought, whereas *AcCIPK9.3* expression was significantly upregulated. The expression of *AcCIPK10.3* and *AcCIPK10.4* showed no significant change.

It is noteworthy that *AcCIPK24.5* and *AcCBL10*, which are highly conserved in phylogeny and whose homologs in Arabidopsis are known to interact, exhibited both correlated and specific expression patterns in response to drought stress. On one hand, their expression trends were consistent in root and stem tissues, both being suppressed by drought. On the other hand, in cladode tissues, *AcCIPK24.5* expression was inhibited by drought, while *AcCBL10* expression was significantly induced. This differential, even opposite, transcriptional response to the same stress signal in cladode tissues suggests that these two genes may be regulated by distinct upstream factors, indicating a complex functional relationship.

3.8 Interaction between AcCIPK24 and AcCBL10

Given the conserved homology and coordinated yet distinct expression patterns under stress, we hypothesized that AcCIPK24 and AcCBL10 might physically interact to form a functional module. This interaction was tested using a yeast two-hybrid (Y2H) assay. The constructs pGBKT7-AcCIPK24 and pGADT7-AcCBL10 were co-transformed into the yeast strain Y2HGold. As shown in Figure 3, the co-transformants grew robustly on SD/-Trp-Leu-His selective medium across serial dilutions 10 to 10^{-3}, with growth comparable to that of the positive control (pGADT7-T + pGBKT7-P53). In contrast, the two negative controls (pGADT7-T + pGBKT7-Lam and pGBKT7-AcCIPK24 + empty pGADT7) showed almost no colony formation under the same selective conditions. These results indicate that AcCIPK24 and AcCBL10 specifically interact in yeast cells, and that this interaction is not due to autoactivation or nonspecific binding of either protein alone.

3.9 Effects of Drought Stress and Exogenous ABA Treatment on Endogenous ABA Content in Plants

To investigate whether ABA signaling is involved in the response of *A. cochinchinensis* to drought stress and to elucidate its potential regulatory mode, we first measured the dynamic changes in endogenous ABA content in plants under PEG6000 simulated drought conditions. Subsequently, we analyzed the feedback regulation of exogenous ABA on endogenous ABA homeostasis. Under PEG6000 simulated drought stress, the endogenous ABA content in *A. cochinchinensis* plants exhibited a dynamic pattern of initial increase followed by a slight decrease over time. Compared to the 0-hour control, ABA content increased significantly ($P < 0.05$) at 3 hours of stress treatment, peaked at 6 hours ($P < 0.001$), and although slightly decreased by 12 hours, it remained significantly higher than the control level ($P < 0.001$) (Fig 4A). This indicates that drought stress effectively activates ABA biosynthesis or accumulation in *A. cochinchinensis*.

To further explore the role of ABA signaling in this process, exogenous ABA was applied in combination with PEG6000 treatment. The introduction of exogenous ABA significantly altered the accumulation dynamics of endogenous ABA. Compared to the drought-only treatment group (Fig 4A), plants subjected to combined PEG and ABA treatment exhibited a higher basal ABA level even at 0 hours. After 3 hours of stress treatment, their endogenous ABA content rapidly reached its highest value ($P < 0.001$), and the timing of this peak occurred significantly earlier than in the drought-only group (6 hours). At 6 and 12 hours, endogenous ABA content gradually declined but remained significantly higher than the control ($P < 0.001$) (Fig 4B). This suggests that exogenous ABA potentiates the drought-induced ABA response, possibly via a positive feedback mechanism.

Discussion

The calcium signaling network is a core regulatory system for plant responses to environmental stress. The CBL-CIPK module, as a key calcium signal decoder, converts intracellular calcium signals into downstream physiological responses through specific interactions (Batistič and Kudla, 2012; Weinl & Kudla, 2009). Based on the full-length transcriptome and expression analysis of *A. cochinchinensis*, this study systematically analyzed the molecular characteristics and expression patterns of its CBL-CIPK network under drought stress, providing experimental evidence for understanding the adaptation mechanisms of medicinal plants in karst habitats.

Phylogenetic analysis revealed that the CBL and CIPK family members in *A. cochinchinensis* exhibit both conservation and diversity in evolution. AcCIPK24 and AcCBL10 clustered into the same branch as the core components of the Arabidopsis SOS pathway, AtCIPK24/SOS2 and AtCBL10/SOS3, respectively (Fig. 1), suggesting functional conservation of this interaction module in regulating ion homeostasis in dicotyledonous plants (Halfter et al., 2000). Notably, this study identified the presence of alternatively spliced variants of *AcCIPK24.5*, whose structural differences may be involved in the fine-tuning of signaling pathways. Similar phenomena have been reported for Arabidopsis CIPK3 (Liu et al., 2022; Sanyal et al., 2021), implying that the "one gene, multiple transcripts" strategy may be a common mechanism for plants to adapt to complex environments. Considering the karst habitat background of *A. cochinchinensis*, the structural diversity of this network may be related to the selective pressure from periodic drought.

Expression pattern analysis revealed significant tissue specificity and differential stress responses among CBL-CIPK members. Under drought treatment, the expression of AcCIPK24.5 and AcCBL10 was suppressed in roots and stems, while showing differential regulation in cladodes: AcCIPK24.5 was downregulated, whereas AcCBL10 was significantly upregulated (Figs. 2 and 3). This expression decoupling phenomenon indicates that the transcriptional regulation of *CBL* and *CIPK* is not simply coordinated but follows a tissue-specific regulatory logic. Considering that cladodes are the main photosynthetic and water exchange organs in *A. cochinchinensis*, the specific induction of *AcCBL10* may be involved in local regulation of stomatal behavior or photosynthetic protection. This aligns with functional reports on SlCBL1 in tomato leaves (Sanyal et al., 2017; Kolukisaoglu et al., 2004), suggesting that CBL members may play specific roles in optimizing water use efficiency in photosynthetic tissues.

Further analysis, combined with hormone treatment and endogenous hormone determination results (Fig. 4), revealed that exogenous ABA significantly induced the expression of *AcCBL10* and *AcCIPK24.5* while promoting endogenous ABA accumulation with an earlier peak. This result suggests a functional association between the CBL-CIPK module and the ABA signaling pathway, potentially forming a coordinated response loop, the CBL-CIPK complex may act both as a downstream effector unit of ABA signaling and participate in the regulation of ABA dynamic accumulation through feedback modulation (Zhu et al., 2007). Furthermore, endogenous ABA under drought stress exhibited a dynamic change of first increasing then decreasing. This pulsatile response may help plants initiate stress defense while avoiding excessive growth inhibition caused by sustained high ABA levels, reflecting a strategy of temporally precise regulation in stress responses.

In summary, based on the available experimental evidence, this study proposes that in *A. cochinchinensis*, drought signals may activate the AcCBL10-AcCIPK24 interaction module, coordinating with the ABA pathway to achieve spatiotemporal regulation of stress responses. The differential expression of this network in roots/stems versus cladodes may serve to maintain ion homeostasis and protect photosynthetic organs, respectively, collectively supporting its adaptive capacity in the karst drought environment. This work not only expands the understanding of the CBL-CIPK network in non-model medicinal plants but also provides a reference case for deciphering the molecular basis of plant environmental adaptation.

Declarations

Consent for publication

Not applicable.

Availability of data and materials

All data sheets and codes to process data are available upon request to the corresponding author, miaoliu (miaoliu1991@163.com).

Competing interests

The authors declare that they have no competing interests.

Funding

This work was supported by the National Natural Science Foundation of China (32360487); Department of Science and Technology of Guizhou Province (Qiankehe Fundamentals ZK [2023] General 114). Modern Industrial Technology System of Traditional Chinese Medicine in Guizhou Province (GZCYTX2024).

Authors' contributions

Liu Miao and Ming-sheng Zhang: conceptualization, methodology and funding acquisition, **Zheng-xi Long, and Liu Tang:** analysis, validation, **Sheng-bo Lu and Yu-ting Yang:** writing-original draft preparation, **Liu Miao and Zheng-xi Long:** discussion, writing-reviewing and editing, All authors read and approved the final manuscript.

References

1. **Apse MP, Aharon GS, Snedden WA, Blumwald E.** Salt tolerance conferred by overexpression of a vacuolar Na^+/H^+ antiport in Arabidopsis. Science. 1999 Aug 20;285(5431):1256-8. doi: 10.1126/science.285.5431.1256.
2. **Arab M, Najafi Zarrini H, Nematzadeh G, Heidari P, Hashemipetroudi SH, Kuhlmann M.** Comprehensive Analysis of Calcium Sensor Families, CBL and CIPK, in Aeluropus littoralis and Their Expression Profile in Response to Salinity. Genes (Basel). 2023 Mar 20;14(3):753. doi: 10.3390/genes14030753.
3. **Aslam M, Fakher B, Jakada BH, Zhao L, Cao S, Cheng Y, Qin Y.** Genome-Wide Identification and Expression Profiling of CBL-CIPK Gene Family in Pineapple (*Ananas comosus*) and the Role of AcCBL1 in Abiotic and Biotic Stress Response. Biomolecules. 2019 Jul 20;9(7):293. doi: 10.3390/biom9070293.
4. **Batistic O, Kudla J.** Integration and channeling of calcium signaling through the CBL calcium sensor/CIPK protein kinase network. Planta. 2004 Oct;219(6):915-24. doi: 10.1007/s00425-004-1333-3.
5. **Biasini M, Bienert S, Waterhouse A, Arnold K, Studer G, Schmidt T, Kiefer F, Gallo Cassarino T, Bertoni M, Bordoli L, Schwede T.** SWISS-MODEL: modelling protein tertiary and quaternary structure using evolutionary information. Nucleic Acids Res. 2014 Jul;42(Web Server issue):W252-8. doi: 10.1093/nar/gku340. Epub 2014 Apr 29.

6. **Chao M, Dong J, Hu G, Ren R, Huang L, Li Y, Zhang J, Wang Q.** Sequence Characteristics and Expression Analysis of GhCIPK23 Gene in Upland Cotton (*Gossypium hirsutum* L.). Int J Mol Sci. 2022 Oct 10;23(19):12040. doi: 10.3390/ijms231912040.
7. **Cheng YW, Chen YM, Zhao QQ, Zhao X, Wu YR, Chen DZ, Liao LD, Chen Y, Yang Q, Xu LY, Li EM, Xu JZ.** Long Read Single-Molecule Real-Time Sequencing Elucidates Transcriptome-Wide Heterogeneity and Complexity in Esophageal Squamous Cells. Front Genet. 2019 Oct 4;10:915. doi: 10.3389/fgene.2019.00915.
8. **Cheong YH, Pandey GK, Grant JJ, Batistic O, Li L, Kim BG, Lee SC, Kudla J, Luan S.** Two calcineurin B-like calcium sensors, interacting with protein kinase CIPK23, regulate leaf transpiration and root potassium uptake in Arabidopsis. Plant J. 2007 Oct;52(2):223-39. doi: 10.1111/j.1365-313X.2007.03236.x.
9. **Cho JH, Choi MN, Yoon KH, Kim KN.** Ectopic Expression of SjCBL1, Calcineurin B-Like 1 Gene From Sedirea japonica, Rescues the Salt and Osmotic Stress Hypersensitivity in Arabidopsis cbl1 Mutant. Front Plant Sci. 2018 Aug 21;9:1188. doi: 10.3389/fpls.2018.01188.
10. **Conesa A, Götz S, García-Gómez JM, Terol J, Talón M, Robles M.** Blast2GO: a universal tool for annotation, visualization and analysis in functional genomics research. Bioinformatics. 2005 Sep 15;21(18):3674-6. doi: 10.1093/bioinformatics/bti610. Epub 2005 Aug 4. PMID: 16081474.
11. **Duan Y, Zhang W, Cheng Y, Shi M, Xia XQ.** A systematic evaluation of bioinformatics tools for identification of long noncoding RNAs. RNA. 2021 Jan;27(1):80-98. doi: 10.1261/rna.074724.120. Epub 2020 Oct 14.
12. **Gao Y, Zhang G.** A calcium sensor calcineurin B-like 9 negatively regulates cold tolerance via calcium signaling in Arabidopsis thaliana. Plant Signal Behav. 2019;14(3):e1573099.
13. **González EM.** Drought Stress Tolerance in Plants. Int J Mol Sci. 2023 Mar 31;24(7):6562. doi: 10.3390/ijms24076562.
14. **Hajihashemi S, Noedoost F, Geuns JMC, Djalovic I, Siddique KHM.** Effect of Cold Stress on Photosynthetic Traits, Carbohydrates, Morphology, and Anatomy in Nine Cultivars of Stevia rebaudiana. Front Plant Sci. 2018 Sep 28;9:1430. doi: 10.3389/fpls.2018.01430.
15. **Halfter U, Ishitani M, Zhu JK.** The Arabidopsis SOS2 protein kinase physically interacts with and is activated by the calcium-binding protein SOS3. Proc Natl Acad Sci U S A. 2000 Mar 28;97(7):3735-40. doi: 10.1073/pnas.97.7.3735.
16. **Huang D, Mao Y, Guo G, Ni D, Chen L.** Genome-wide identification of PME gene family and expression of candidate genes associated with aluminum tolerance in tea plant (*Camellia sinensis*). BMC Plant Biol. 2022 Jun 24;22(1):306. doi: 10.1186/s12870-022-03686-7.
17. **Huang S, Zhang H, Chen W, Wang J, Wu Z, He M, Zhang J, Hu X, Xiang S.** Screening of Tnfaip1-Interacting Proteins in Zebrafish Embryonic cDNA Libraries Using a Yeast Two-Hybrid System. Curr Issues Mol Biol. 2023 Oct 10;45(10):8215-8226. doi: 10.3390/cimb45100518.
18. **Kanwar P, Sanyal SK, Tokas I, Yadav AK, Pandey A, Kapoor S, Pandey GK.** Comprehensive structural, interaction and expression analysis of CBL and CIPK complement during abiotic stresses and development in rice. Cell Calcium. 2014 Aug; 56(2):81-95. doi: 10.1016/j.ceca.2014.05.003.
19. **Kaya C, Uğurlar F, Adamakis IS.** Molecular Mechanisms of CBL-CIPK Signaling Pathway in Plant Abiotic Stress Tolerance and Hormone Crosstalk. Int J Mol Sci. 2024 May 6;25(9):5043. doi: 10.3390/ijms25095043.
20. **Kolukisaoglu U, Weinl S, Blazevic D, Batistic O, Kudla J.** Calcium sensors and their interacting protein kinases: genomics of the Arabidopsis and rice CBL-CIPK signaling networks. Plant Physiol. 2004 Jan;134(1):43-58. doi: 10.1104/pp.103.033068.
21. **Lara A, Ródenas R, Andrés Z, Martínez V, Quintero FJ, Nieves-Cordones M, Botella MA, Rubio F.** Arabidopsis K+ transporter HAK5-mediated high-affinity root K+ uptake is regulated by protein kinases CIPK1 and CIPK9. J Exp Bot. 2020 Aug 6;71(16):5053-5060. doi: 10.1093/jxb/eraa212.
22. **Li X, Zou S, Li Z, Cai G, Chen B, Wang P, Dong W.** The identification of human aldo-keto reductase AKR7A2 as a novel cytoglobin-binding partner. Cell Mol Biol Lett. 2016 Oct 24;21:25. doi: 10.1186/s11658-016-0026-9.

23. **Liu XX, Guo QH, Xu WB, Liu P, Yan K.** Rapid Regulation of Alternative Splicing in Response to Environmental Stresses. Front Plant Sci. 2022 Mar 4;13:832177. doi: 10.3389/fpls.2022.832177.
24. **Ma QJ, Sun MH, Lu J, Kang H, You CX, Hao YJ.** An apple sucrose transporter MdSUT2.2 is a phosphorylation target for protein kinase MdCIPK22 in response to drought. Plant Biotechnol J. 2019 Mar;17(3):625-637. doi: 10.1111/pbi.13003. Epub 2018 Oct 2.
25. **Ma X, Li QH, Yu YN, Qiao YM, Haq SU, Gong ZH.** The CBL-CIPK Pathway in Plant Response to Stress Signals. Int J Mol Sci. 2020 Aug 7;21(16):5668. doi: 10.3390/ijms21165668.
26. **Ning L, Xu Y, Luo L, Gong L, Liu Y, Wang Z, Wang W.** Integrative analyses of metabolome and transcriptome reveal the dynamic accumulation and regulatory network in rhizomes and fruits of *Polygonatum cyrtonema* Hua. BMC Genomics. 2024 Jul 19;25(1):706. doi: 10.1186/s12864-024-10608-4.
27. **Peng Q, Zhu C, Liu T, Zhang S, Feng S, Wu C.** Phosphorylation of OsFD1 by OsCIPK3 promotes the formation of RFT1-containing florigen activation complex for long-day flowering in rice. Mol Plant. 2021 Jul 5;14(7):1135-1148. doi: 10.1016/j.molp.2021.04.003.
28. **Ramos TAR, Galindo NRO, Arias-Carrasco R, da Silva CF, Maracaja-Coutinho V, do Rêgo TG.** RNAmining: A machine learning stand-alone and web server tool for RNA coding potential prediction. F1000Res. 2021 Apr 26;10:323. doi: 10.12688/f1000research.52350.2.
29. **Sanyal SK, Kanwar P, Samtani H, Kaur K, Jha SK, Pandey GK.** Alternative Splicing of CIPK3 Results in Distinct Target Selection to Propagate ABA Signaling in Arabidopsis. Front Plant Sci. 2017 Nov 24;8:1924. doi: 10.3389/fpls.2017.01924.
30. **Shi S, An L, Mao J, Aluko OO, Ullah Z, Xu F, Liu G, Liu H, Wang Q.** The CBL-Interacting Protein Kinase NtCIPK23 Positively Regulates Seed Germination and Early Seedling Development in Tobacco (*Nicotiana tabacum* L.). Plants (Basel). 2021 Feb 8;10(2):323. doi: 10.3390/plants10020323.
31. **Sun J, Chen T, Tao J.** Single molecule, full-length transcript sequencing provides insight into the TPS gene family in Paeonia ostii. PeerJ. 2021 Jul 15;9:e11808. doi: 10.7717/peerj.11808.
32. **Tandon G, Jaiswal S, Iquebal MA, Rai A, Kumar D.** Whole Genome Wide SSR Markers Identification Based on ddRADseq Data. Methods Mol Biol. 2023;2638:59-66. doi: 10.1007/978-1-0716-3024-2_5.
33. **Tang RJ, Wang C, Li K, Luan S.** The CBL-CIPK Calcium Signaling Network: Unified Paradigm from 20 Years of Discoveries. Trends Plant Sci. 2020 Jun;25(6):604-617. doi: 10.1016/j.tplants.2020.01.009. .
34. **Tang RJ, Zhao FG, Garcia VJ, Kleist TJ, Yang L, Zhang HX, Luan S.** Tonoplast CBL-CIPK calcium signaling network regulates magnesium homeostasis in Arabidopsis. Proc Natl Acad Sci U S A. 2015 Mar 10;112(10):3134-9. doi: 10.1073/pnas.1420944112.
35. **Verma P, Sanyal SK, Pandey GK.** Ca2+-CBL-CIPK: a modulator system for efficient nutrient acquisition. Plant Cell Rep. 2021 Nov;40(11):2111-2122. doi: 10.1007/s00299-021-02772-8.
36. **Waadt R, Schmidt LK, Lohse M, Hashimoto K, Bock R, Kudla J.** Multicolor bimolecular fluorescence complementation reveals simultaneous formation of alternative CBL/CIPK complexes in planta. Plant J. 2008 Nov;56(3):505-16. doi: 10.1111/j.1365-313X.2008.03612.x.
37. **Wang L, Feng X, Yao L, Ding C, Lei L, Hao X, Li N, Zeng J, Yang Y, Wang X.** Characterization of CBL-CIPK signaling complexes and their involvement in cold response in tea plant. Plant Physiol Biochem. 2020 Sep;154:195-203. doi: 10.1016/j.plaphy.2020.06.005.
38. **Wang M, Wang S, Hu W, Wang Z, Yang B, Kuang H.** *Asparagus cochinchinensis*: A review of its botany, traditional uses, phytochemistry, pharmacology, and applications. Front Pharmacol. 2022 Nov 30;13:1068858. doi: 10.3389/fphar.2022.1068858.
39. **Wang X, Ouyang L, Chen W, Cao Y, Zhang L.** Efficient expansion and delayed senescence of hUC-MSCs by microcarrier-bioreactor system. Stem Cell Res Ther. 2023 Oct 4;14(1):284. doi: 10.1186/s13287-023-03514-1.

40. **Weinl S, Kudla J.** The CBL-CIPK Ca(2+)-decoding signaling network: function and perspectives. New Phytol. 2009 Nov;184(3):517-528. doi: 10.1111/j.1469-8137.2009.02938.x.
41. **Weinl S, Kudla J.** The CBL-CIPK Ca(2+)-decoding signaling network: function and perspectives. New Phytol. 2009 Nov;184(3):517-528. doi: 10.1111/j.1469-8137.2009.02938.x. PMID: 19860013.
42. **Wu J, Jiang Y, Liang Y, Chen L, Chen W, Cheng B.** Expression of the maize MYB transcription factor ZmMYB3R enhances drought and salt stress tolerance in transgenic plants. Plant Physiol Biochem. 2019 Apr;137:179-188. doi: 10.1016/j.plaphy.2019.02.010. Epub 2019 Feb 15. PMID: 30798172.
43. **Wu X, Zhou C, Li X, Lin J, Aguila LCR, Wen F, Wang L.** Genome-wide identification and immune response analysis of mitogen-activated protein kinase cascades in tea geometrid, Ectropis grisescens Warren (*Geometridae, Lepidoptera*). BMC Genomics. 2023 Jun 22;24(1):344. doi: 10.1186/s12864-023-09446-7.
44. **Wu Y, Feng J, Zhang Q, Wang Y, Guan Y, Wang R, Shi F, Zeng F, Wang Y, Chen M, Chang J, He G, Yang G, Li Y.** Integrative gene duplication and genome-wide analysis as an approach to facilitate wheat reverse genetics: An example in the *TaCIPK* family. J Adv Res. 2024 Jul;61:19-33. doi: 10.1016/j.jare.2023.09.005.
45. **Xiaolin Z, Baoqiang W, Xian W, Xiaohong W.** Identification of the CIPK-CBL family gene and functional characterization of CqCIPK14 gene under drought stress in quinoa. BMC Genomics. 2022 Jun 16;23(1):447. doi: 10.1186/s12864-022-08683-6.
46. **Xu J, Li HD, Chen LQ, Wang Y, Liu LL, He L, Wu WH.** A protein kinase, interacting with two calcineurin B-like proteins, regulates K+ transporter AKT1 in Arabidopsis. Cell. 2006 Jun 30;125(7):1347-60. doi: 10.1016/j.cell.2006.06.011.
47. **Yang H, Tan Y, Zhang T, Tang L, Wang J, Ke Y, Guo Z, Yang X, Yang R, Du Z.** Identification of novel protein-protein interactions of Yersinia pestis type III secretion system by yeast two hybrid system. PLoS One. 2013;8(1):e54121. doi: 10.1371/journal.pone.0054121. Epub 2013 Jan 22.
48. **Yao C, Li W, Liang X, Ren C, Liu W, Yang G, Zhao M, Yang T, Li X, Han D.** Molecular Cloning and Characterization of MbMYB108, a Malus baccata MYB Transcription Factor Gene, with Functions in Tolerance to Cold and Drought Stress in Transgenic Arabidopsis thaliana. Int J Mol Sci. 2022 Apr 27;23(9):4846. doi: 10.3390/ijms23094846.
49. **Yao H, Wang F, Bi Q, Liu H, Liu L, Xiao G, Zhu J, Shen H, Li H.** Combined Analysis of Pharmaceutical Active Ingredients and Transcriptomes of Glycyrrhiza uralensis Under PEG6000-Induced Drought Stress Revealed Glycyrrhizic Acid and Flavonoids Accumulation via JA-Mediated Signaling. Front Plant Sci. 2022 Jun 13;13:920172. doi: 10.3389/fpls.2022.920172.
50. **Ye J, Zhang Y, Cui H, Liu J, Wu Y, Cheng Y, Xu H, Huang X, Li S, Zhou A, Zhang X, Bolund L, Chen Q, Wang J, Yang H, Fang L, Shi C.** WEGO 2.0: a web tool for analyzing and plotting GO annotations, 2018 update. Nucleic Acids Res. 2018 Jul 2;46(W1):W71-W75. doi: 10.1093/nar/gky400.
51. **Yu Q, An L, Li W.** The CBL-CIPK network mediates different signaling pathways in plants. Plant Cell Rep. 2014 Feb;33(2):203-14. doi: 10.1007/s00299-013-1507-1.
52. **Yunmam S, Lee HR, Hong SM, Kim JY, Kang TH, Lee AY, Jang DS, Kim SY.** Aspacochioside C from *Asparagus cochinchinensis* attenuates eumelanin synthesis via inhibition of TRP2 expression. Sci Rep. 2023 Sep 8;13(1):14831. doi: 10.1038/s41598-023-41248-5.
53. **Zhang X, Li X, Zhao R, Zhou Y, Jiao Y.** Evolutionary strategies drive a balance of the interacting gene products for the CBL and CIPK gene families. New Phytol. 2020 Jun;226(5):1506-1516. doi: 10.1111/nph.16445.
54. **Zhang XX, Ren XL, Qi XT, Yang ZM, Feng XL, Zhang T, Wang HJ, Liang P, Jiang QY, Yang WJ, Fu Y, Chen M, Fu ZX, Xu B.** Evolution of the CBL and CIPK gene families in Medicago: genome-wide characterization, pervasive duplication, and expression pattern under salt and drought stress. BMC Plant Biol. 2022 Nov 3;22(1):512. doi: 10.1186/s12870-022-03884-3.
55. **Zheng Y, Jiao C, Sun H, Rosli HG, Pombo MA, Zhang P, Banf M, Dai X, Martin GB, Giovannoni JJ, Zhao PX, Rhee SY, Fei Z.** iTAK: A Program for Genome-wide Prediction and Classification of Plant Transcription Factors, Transcriptional

Regulators, and Protein Kinases. Mol Plant. 2016 Dec 5;9(12):1667-1670. doi: 10.1016/j.molp.2016.09.014. Epub 2016 Oct 5. PMID: 27717919.

56. **Zhou L, Lan W, Chen B, Fang W, Luan S.** A calcium sensor-regulated protein kinase, CALCINEURIN B-LIKE PROTEIN-INTERACTING PROTEIN KINASE19, is required for pollen tube growth and polarity. Plant Physiol. 2015 Apr;167(4):1351-60. doi: 10.1104/pp.114.256065.
57. **Zhu K, Fan P, Liu H, Tan P, Ma W, Mo Z, Zhao J, Chu G, Peng F.** Insight into the CBL and CIPK gene families in pecan (Carya illinoinensis): identification, evolution and expression patterns in drought response. BMC Plant Biol. 2022 Apr 28;22(1):221. doi: 10.1186/s12870-022-03601-0.
58. **Zhu SY, Yu XC, Wang XJ, Zhao R, Li Y, Fan RC, Shang Y, Du SY, Wang XF, Wu FQ, Xu YH, Zhang XY, Zhang DP.** Two calcium-dependent protein kinases, CPK4 and CPK11, regulate abscisic acid signal transduction in Arabidopsis. Plant Cell. 2007 Oct;19(10):3019-36. doi: 10.1105/tpc.107.050666. Epub 2007 Oct 5.

Figures

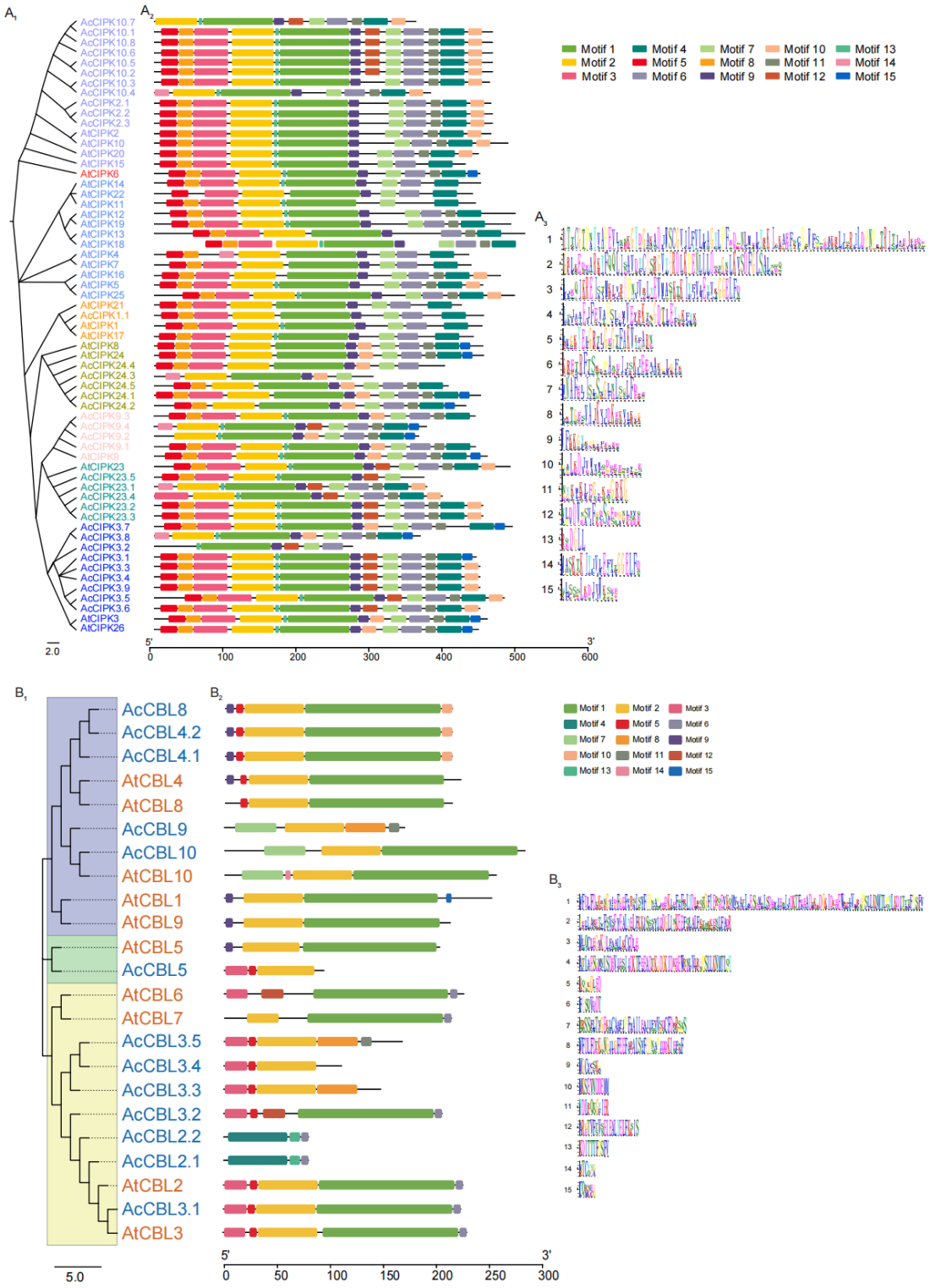

Figure 1

Phylogenetic relationships, motif of CBL and CIPK proteins in Arabidopsis and *A. cochinchinensis*, the amino acid sequences of AtCBL and AcCBL, AtCIPK and AcCIPK were aligned using ClustalW2. (A_1) Phylogenetic analysis of CIPK proteins in in Arabidopsis and *A. cochinchinensis*. (B_1) Phylogenetic analysis of CBL proteins in in Arabidopsis and *A. cochinchinensis*. The phylogenetic tree is constructed by MEGA 12 using the neighbor-joining method with 1000 bootstrap replicates and displayed using FigTree v1.4.0. At: Arabidopsis; Ac: *A. cochinchinensis*. (B_1) Conservative motifs of AtCIPK

and AcCIPK proteins identifed by MEME. (B_2) Conservative motifs of AtCBL and AcCBL proteins identifed by MEME. The motifs were indicated by colored boxes and their numbers are shown in the scale the diagram.

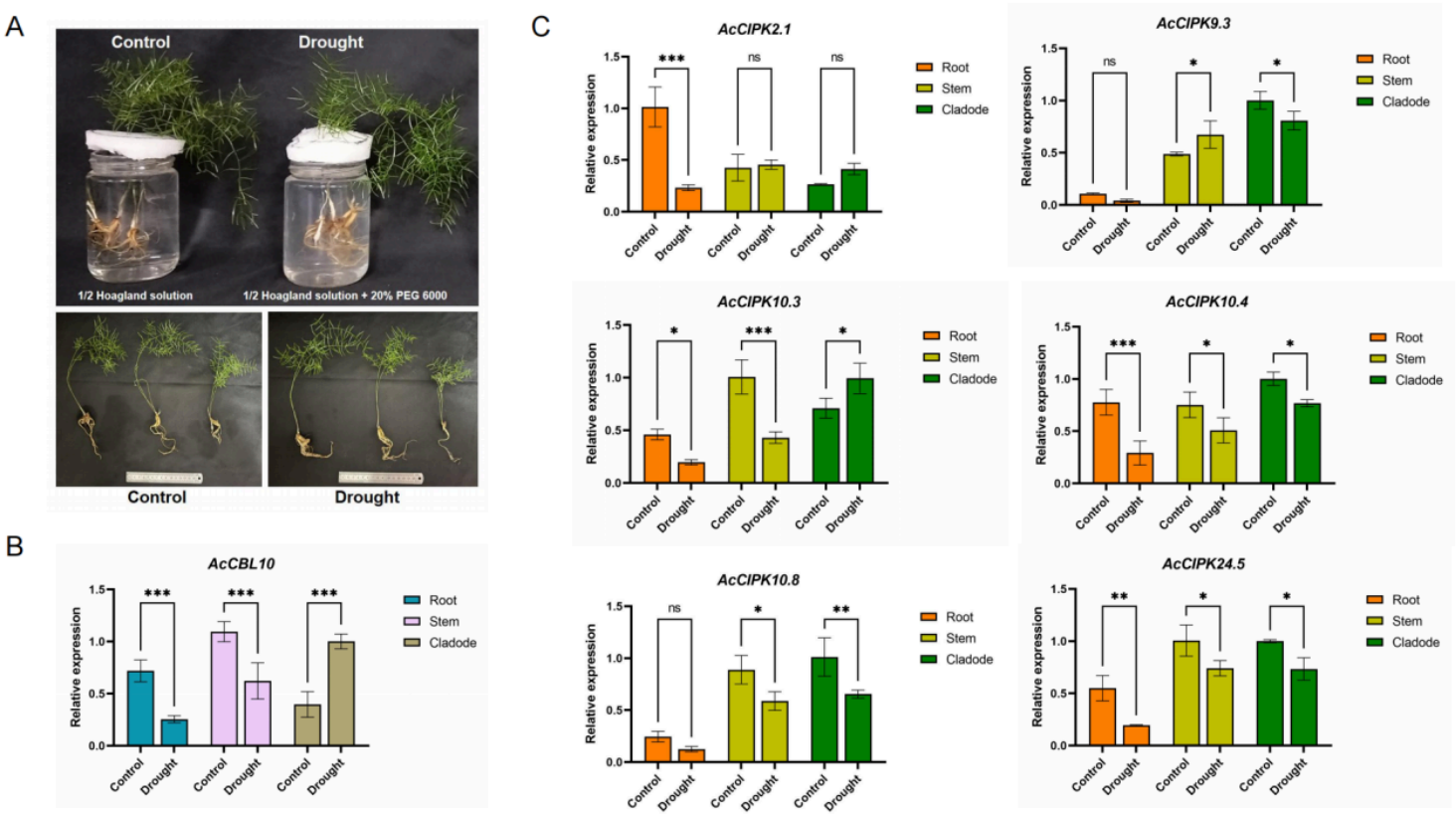

Figure 2

Morphological and Specific Gene Expression Responses of *A. cochinchinensis* to Drought Stress. (A) Morphology of *A. cochinchinensis* after 3 days of drought stress. (B) Relative expression analysis of *AcCBL10* under drought stress at 0, 3, 6, and 12 h.(C) Relative expression analysis of *AcCIPK* under drought stress at 0, 3, 6, and 12 h. CK: 0 h drought stress (control). ** denotes a significant difference at $P < 0.01$, as determined using Student's t test, Bars represent SD of the average, mean ± SD.

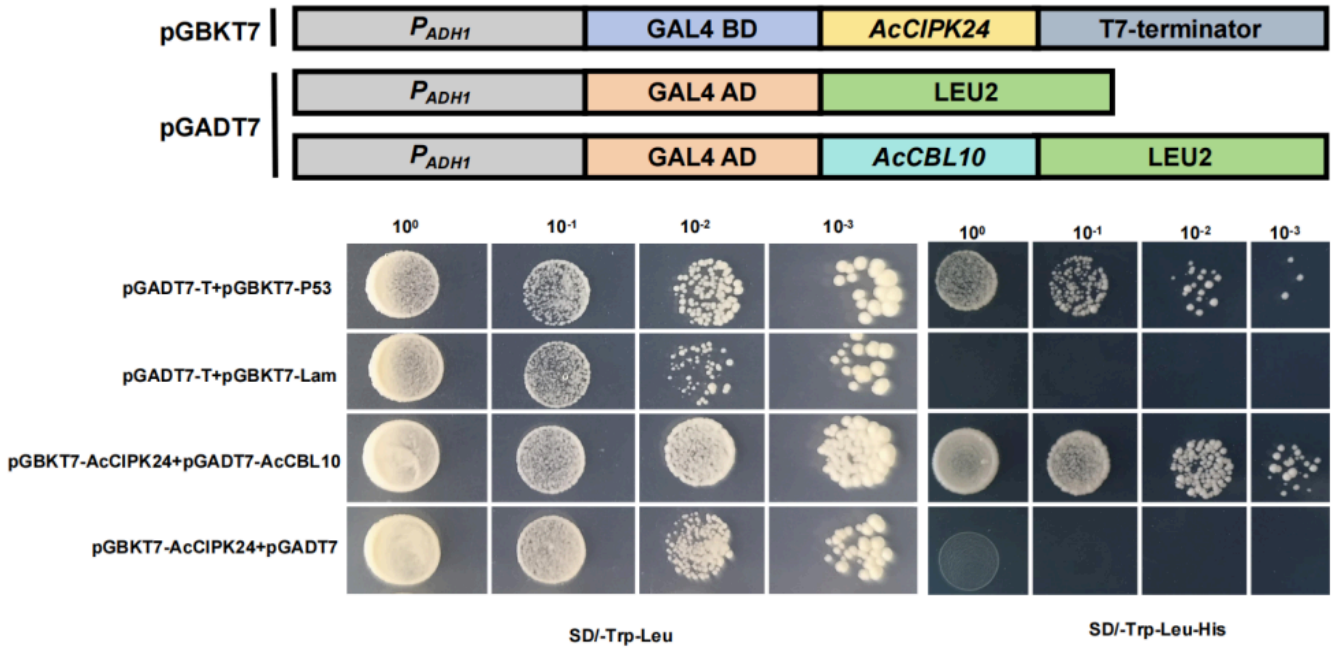

Figure 3

Yeast-two-hybrid (Y2H) validation of the interaction between AcCBL10 and AcCIPK24. Positive control: pGBKT7-p53 + pGADT7-T; negative control: pGBKT7-Lam + pGADT7-T. The rest are experimental groups.

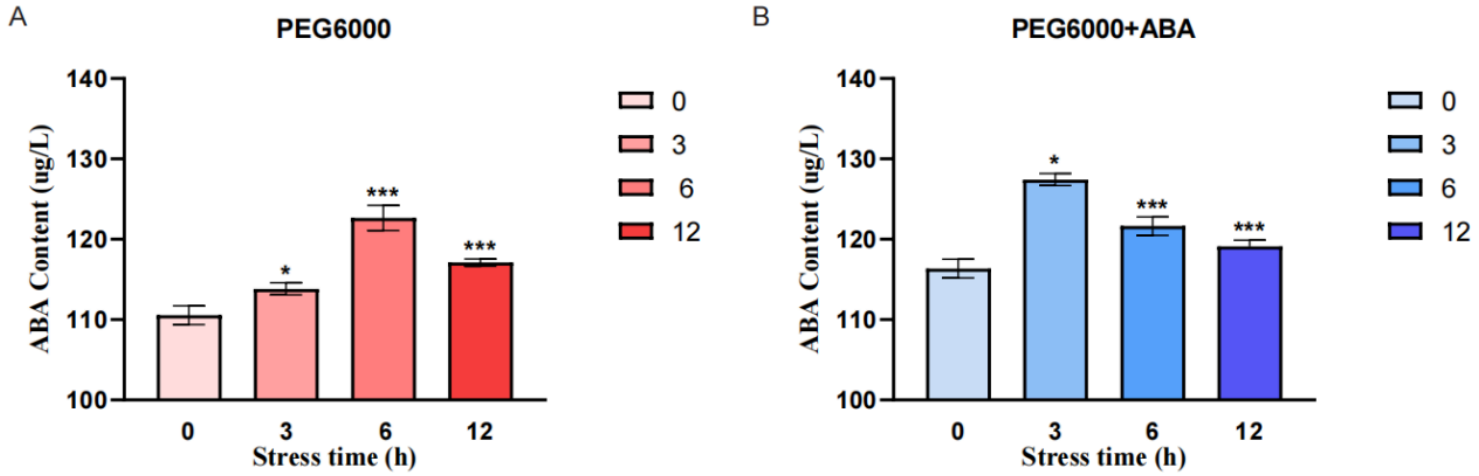

Figure 4

Effects of PEG 6000 and ABA treatments on ABA content in cladodes of *A. cochinchinensis*. (A) Changes in endogenous ABA content in cladodes after treatment with 20% (w/v) PEG 6000. (B) Changes in ABA content in cladodes under combined treatment with 20% PEG 6000 and 100 mM ABA.Samples were collected at 0, 3, 6, and 12 h after treatment. Data are presented as mean ± SD of at least three biological replicates. Statistical significance was determined by one-way ANOVA (*P < 0.05, **P < 0.01, ***P < 0.001).

Supplementary Files

This is a list of supplementary files associated with this preprint. Click to download.

- TableS1.docx
- Supplementarypictures.docx